

An Online Implementation of the Panoramic ECAP Method for Estimating Patterns of Current Spread and Neural Responsiveness in Cochlear Implant Users

Charlotte Garcia 

Cambridge Hearing Group, MRC Cognition & Brain Sciences Unit, University of Cambridge, Cambridge, United Kingdom.

 OPEN ACCESS

PEER REVIEWED

ARTÍCULO ORIGINAL

DOI: 10.51445/sja.auditio.vol10.2026.128

Received: 24 . 11 . 2025

Reviewed: 31 . 12 . 2025

Accepted: 06 . 04 . 2026

Published: 23 . 06 . 2026

Edited by:

Miriam Isabel Marrufo Pérez 

Universidad de Salamanca, Spain.

Reviewed by:

Chris James

Cochlear France SAS, Toulouse, France.

Evelien De Groote 

KU Leuven, Belgium.

Norbert Dillier 

Universitätsspital Zürich, Switzerland.

How to cite:

Garcia, C. (2026). An Online Implementation of the Panoramic ECAP Method for Estimating Patterns of Current Spread and Neural Responsiveness in Cochlear Implant Users. *Auditio*, 10, e128. <https://doi.org/10.51445/sja.auditio.vol10.2026.128>

Correspondence

Charlotte Garcia

MRC Cognition & Brain Sciences Unit, 15 Chaucer Road, Cambridge, CB2 7EF, United Kingdom.

Email: Charlotte.Garcia@mrc-cbu.cam.ac.uk

  CC-BY 4.0

© 2026 Los autores / The authors

<https://journal.auditio.com/>

Publicación de la Asociación Española de Audiología (AEDA)

Abstract

The Panoramic ECAP Method (PECAP) is a research tool that leverages objective measurements of neural responses to a cochlear implant (electrically evoked compound action potentials, or ECAPs) to provide detailed estimates of neural-activation patterns along the length of the implanted cochlea. An online implementation of the PECAP tool is presented for use with two devices of the three major cochlear-implant manufacturers. The associated online platform can be used in conjunction with cochlear-implant clinical software to collect PECAP data from users and to analyse the resulting measurements to predict personalised current-spread and neural-responsiveness estimates for each active electrode in the patient's clinical software.

Keywords

Cochlear implant, ECAP, neural health, current spread, objective measures, online implementation.

Findings, Limitations, Perspectives and Considerations

Findings

- PECAP provides patient-specific estimates of neural-activation patterns in cochlear-implant patients.
- PECAP Online demonstrates clinical translatability, increases accessibility, and at the time of publication has 35 users across 12 countries.

Limitations

- Due to limitations in clinical software, PECAP Online only supports data collection in Cochlear devices. Advanced Bionics data can be collected through research interfaces.
- PECAP Online supports analysis from Cochlear and Advanced Bionics Devices.
- PECAP Online does not automatically remove electrical artefacts.

Perspectives

- PECAP Online's accessibility can provide information about patient-specific patterns of neural activation and could support tailored cochlear-implant programming.

Considerations

- PECAP is not yet a validated clinical tool at the time of publication, but can support research initiatives related to characterisation of cochlear-implant electrode-neuron interfaces.
- Future versions of PECAP Online will be compatible with MED-EL devices and Cochlear's NEXA platform.

Background

Cochlear Implants (CIs) are neuro-prosthetic devices that provide a sense of sound to severe- to profoundly-deaf users by bypassing the outer portions of the auditory system and directly stimulating the auditory nerve using a small array of electrodes surgically implanted inside the cochlea (Mudry & Mills, 2013; Zeng, 2022). While many users are able to understand speech well using their devices without the need for additional, non-auditory cues such as lip reading, there is nevertheless a lot of variability in speech-perception outcomes (Blamey et al., 2013; Firszt et al., 2004; Friesen et al., 2001). A key factor that likely limits some cochlear-implant users' ability to achieve their hearing potential with their devices is a sub-optimal electrode-neuron interface (Pfungst et al., 2015). This is the interface between the electrodes of the device and the neighbouring auditory nerve that responds to electrical stimulation from the implant. The health of this auditory nerve and the spread of electrical current within the cochlea are integral to this interface.

Patient-to-patient variability in cochlear geometry (Hrncirik et al., 2022; Swords, 2024), cochlear-implant manufacturer's electrode array geometries (Davis et al., 2016; Garcia & Carlyon, 2025; Jwair et al., 2021), and surgical approaches (Jwair et al., 2022; Wanna et al., 2014) can contribute to differences in electrode-array placement within the cochlea relative to the excited neural populations. Additionally, differences in hearing pathology (He et al., 2018; Moyaert et al., 2025; Skidmore et al., 2021), duration of deafness (Blamey et al., 2013; Holden et al., 2013; Lazard et al., 2012; Ramekers et al., 2022; Wu et al., 2019), and other factors can contribute to variations in the health of the auditory nerve between patients and at different parts of the implanted cochlea. It is possible to identify post-surgical electrode placement using computerised tomography (CT) scans and specialist electrode-modiolus-distance calculation techniques (Mewes et al., 2023; Sismono et al., 2022). However, these techniques are not always common clinical practice due in part to considerations of cost and radiation exposure, and do not necessarily reflect the spread of electrical current from the electrodes at the level of the auditory nerve itself (Garcia & Carlyon, 2025).

The health of the auditory nerve cannot be measured directly in vivo without explanting neural tissue and subsequently employing image-analysis

techniques, a process that would render the tissue unusable after the intervention. However, there have been a myriad of techniques proposed for indirectly measuring various aspects of auditory-nerve health using a mixture of electrophysiological (Brochier et al., 2021; de Vos et al., 2018; DeVries et al., 2016; Garcia et al., 2021; Kim et al., 2017; Konerding et al., 2025; McKay et al., 2013; Prado-Guitierrez et al., 2006; Ramekers et al., 2014) and behavioural/psychophysical (Bierer, 2010; Carlyon et al., 2018; Goldwyn et al., 2010; Kalkman et al., 2022; Peng et al., 2025; Zhou & Pfingst, 2014) techniques.

The present article describes one such electrophysiological technique that provides estimates of both the spread of electrical current and the responsiveness of the auditory nerve along the length of the implanted cochlea for individual patients: the Panoramic ECAP Method (PECAP).

The Panoramic ECAP Method

The PECAP method requires the measurement of a set of electrically evoked compound action potentials (ECAPs). An ECAP is a measure of the synchronous, peripheral neural response of the auditory nerve to a stimulating current pulse delivered by an electrode of the CI (Brown et al., 1990; Charlet de Sauvage et al., 1983). ECAPs are routinely measured in clinical settings, due in part to the relative ease of recording them, as they require no additional measurement hardware beyond that of the clinical device itself. They leverage non-stimulating intra-cochlear electrodes to record the response, and are sometimes used to estimate threshold (T) and comfort (C) levels, although their predictive ability for behavioural reports of loudness has been questioned (de Vos et al., 2018; McKay et al., 2013). Since the responses of the auditory nerve are orders of magnitude smaller than the electrical stimulation artefacts, artefact-reduction paradigms must be employed in order to isolate the neural response (Abbas et al., 1999). The forward-masking artefact-reduction technique isolates the neural response to a probe stimulus by employing multiple recording frames. One frame has a probe pulse that will contain both neural response to the said pulse and its electrical artefact. A second frame contains a masker pulse including both neural response to and electrical artefact from the masker pulse. A third frame contains a probe preceded by a

masker, in which the neural response to the probe is masked by the masker, while the recording frame will still contain the neural response to the masker and both electrical artefacts. A subtraction technique can then be employed to extract the neural response to the probe from the electrical artefacts. The effectiveness of the forward-masking artefact-reduction technique for isolating the neural response to the probe pulse is a function of the efficiency of the masker in suppressing the neural response to the probe. This aspect of the technique has been exploited to measure ‘spread of excitation’ or ‘spatial forward masking’ curves by moving the masker onto different electrodes with increasing distance from the electrode on which the probe is presented (Cohen et al., 2003; Hughes & Stille, 2010). As the masker moves to electrodes farther away from the probe electrode, the amount of neural tissue that is excited by *both* pulses is reduced, and the efficiency of the artefact-reduction technique is also reduced as a function of this reduction in overlap of stimulated neural tissue. However, this approach overlooks the variable contribution of current-spread profiles from different masker electrodes. It interprets the reduction of extractable neural response to the probe with increasing distance of the masker as the pattern of spread of excitation from the probe electrode alone. Subsequent approaches have overcome this limitation by recording ECAPs for every combination of masker and probe electrode and treating each ECAP as reflecting the joint neural excitation patterns produced by both the masker and probe electrodes (Biesheuvel et al., 2016; Cosentino et al., 2015). The revised PECAP method built upon Cosentino *et al.*’s approach to separately parameterise the relative contribution of current spread and neural responsiveness to the neural excitation patterns centred at each electrode (Garcia et al., 2021).

The PECAP method presented by Garcia *et al.* accepts an $n \times n$ measurement matrix M_0 containing the ECAP amplitudes from each combination of masker and probe electrode for the n electrodes switched on in the cochlear-implant user’s clinical programme, recorded at the most-comfortable level (MCL). Within M_0 , $M_{p,m}$ is the amplitude of the ECAP recorded when the probe pulse is delivered on electrode p and the masker pulse is delivered on electrode m ($M_{4,9}$ would indicate the ECAP amplitude for when the probe is presented on electrode 4 and the masker on electrode 9). The algorithm initiates two random vectors σ (current spread) and η (neural

responsiveness) of length n that represent the relative contributions of current spread and neural responsiveness to the neural excitation pattern centred at each electrode. Each cell of σ defines the width of a Gaussian curve that represents the spread of electrical current centred at each electrode, and can therefore be expanded to n Gaussian curves in an $n \times n$ matrix C . Each Gaussian curve of C is then multiplied by the normalising vector η to form the $n \times n$ neural excitation matrix A . As each ECAP amplitude represents the joint neural excitation pattern of the masker and probe electrodes, the underlying measurement matrix M can be inferred from A by multiplying the neural excitation patterns centred at each electrode as shown in equation 1 (note that a cell-by-cell multiplication is employed, not a dot-product):

$$\hat{M} = \sqrt{A^T * A} \quad (1)$$

For example, the ECAP amplitude in cell $M_{4,9}$ of M represents the joint neural excitation profiles from electrodes 4 and 9, or the overlapping neural tissue that is stimulated both by electrode 4 and by electrode 9. Therefore, $M_{4,9}$ can be estimated by multiplying the neural excitation at electrode 9 when electrode 4 is stimulated ($A_{4,9}$) with the neural excitation at electrode 4 when electrode 9 is stimulated ($A_{9,4}$), and by taking the square root, as shown in equation 2. It follows that \hat{M} is inherently symmetrical, and so $M_{4,9}$ is also equivalent to $M_{9,4}$:

$$\hat{M}_{4,9} = \hat{M}_{9,4} = \sqrt{A_{4,9} * A_{9,4}} \quad (2)$$

The PECAP algorithm then employs a nonlinear optimisation technique based on sequential quadratic programming that allows each cell of σ and η to adjust in order to minimise the least squared error between the \hat{M} matrix recreated from the updating the values in each cell of the parameterised σ and η , and the measured M_0 . As the algorithm is an ill-defined inverse problem, biologically realistic hard limits and smoothness constraints are applied to the values in each cell of σ and η to avoid convergence to differing local minima. The final values of σ and η after the convergence of the optimisation loop and the minimisation of the least squared error between M_0 and \hat{M} constitute the outputs of the algorithm.

Ultimately, $\sigma_{1:n}$ contains the widths of the Gaussian curves that represent the current spread centred at electrodes 1 to n , and $\eta_{1:n}$ represents the relative neural responsiveness at electrodes 1 to n . An example of the input data M_0 and output estimates σ and η is included in Figure 1. More details can be found in Garcia, et al. (2021) and Garcia (2022).

Due especially to the parameterised nature of the PECAP algorithm’s output estimates, it was necessary to validate that the measures reflect current spread and neural responsiveness respectively, and that they separate these aspects of the electrode-neuron interface from each other. A first experiment was conducted to investigate the accuracy of the neural-responsiveness estimate. This was primarily done by simulating a localised region of reduced neural responsiveness by selecting a single electrode on which to present two pre-pulses before each frame of the forward-masking ECAP recording paradigm throughout the entirety of the recording of M_0 . This put some of the neural population that responds to electrical stimulation by the targeted electrode into a refractory state throughout the time frame during which those nerves would normally be responding to the masker or probe pulses, creating an artificial and temporary neural ‘more-dead’ region than when compared to the standard M_0 -recording control condition. The results of this experiment demonstrated that the pre-pulse manipulation resulted in lower estimates of neural-responsiveness near the target

electrode than in the control condition (Garcia et al., 2021). The effect was locally restricted to a few electrodes, and had no effect on the current-spread estimate, demonstrating the ability of PECAP to detect local areas of reduced neural responsiveness and to correctly attribute them to η , the neural-responsiveness estimate.

Garcia et al. (2021) also demonstrated a correlation between η and focused thresholds, another measure that has been suggested to predict cochlear neural health (DeVries et al., 2016), suggesting some shared aspect of cochlear neural health that is captured by the two metrics. This correlation was replicated with another similar metric that captures the difference between focused and unfocused thresholds (Peng et al., 2025). However, an electrode-to-electrode variability metric, thought to represent off-site listening calculated from the behavioural threshold measures, predicted phoneme-recognition scores whereas it did not when calculated using PECAP’s η . This suggests that this shared aspect of cochlear neural health captured by the two metrics may not be an aspect that is directly related to speech perception. PECAP’s η has, however, been shown to be more isolated from non-neural factors of the electrode-neuron interface such as the electrode-modiolus distance than another neural-health metric known as the Failure Index (Garcia et al., 2025). It has also been shown to predict speech-perception scores in a larger study (Dawson et al., 2025b, 2025a).

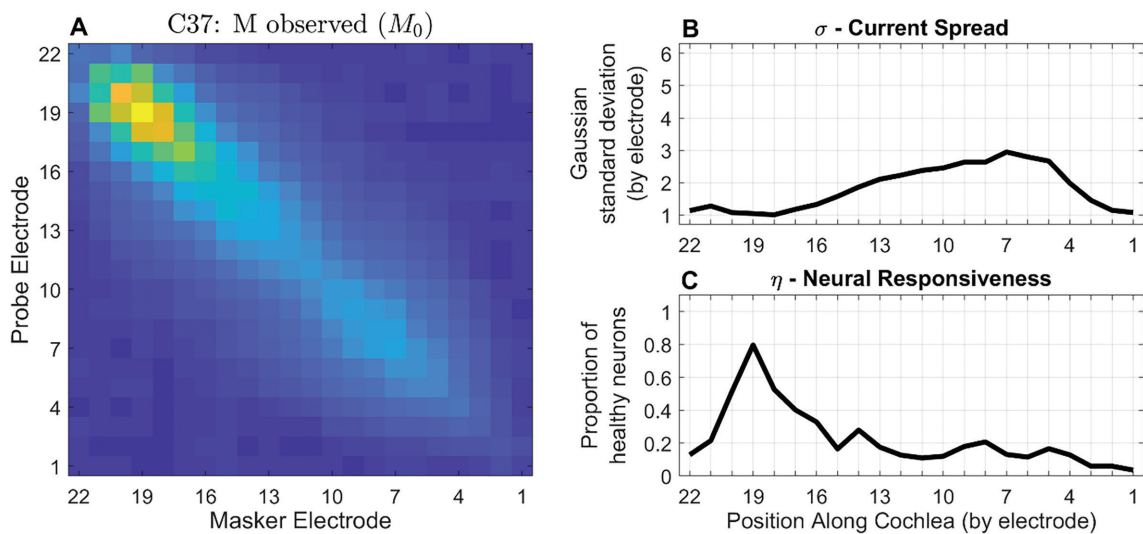


Figure 1. Panoramic ECAP Method example from participant C37 who has a Cochlear CI632 (Slim Modiolar) array. Data was collected at the MRC Cognition & Brain Sciences Unit, University of Cambridge. The M_0 is depicted on the left in panel A, with the current-spread (panel B) and neural-responsiveness (panel C) estimates on the right. Panel A depicts higher ECAP amplitudes in yellow and lower amplitudes in blue. (A colour bar is omitted because the algorithm relies on the relative values of cells in M_0 and not on their absolute values).

The accuracy of PECAP's current-spread estimate (σ) was evaluated using a within-participant study design where the degree of current spread was manipulated. In addition to the standard control-condition paradigm for recording M_0 , a condition was included that selected an electrode on which to present stimulating current not just on the central electrode but for 3 or 5 adjacent electrodes. This technique, referred to as 'blurring', increases the spread of electrical current in the cochlea compared to stimulation using a single electrode at a time, and has been shown to reduce performance on spectro-temporal tests and degrade speech perception when applied at the apex (Goehring et al., 2020, 2021). When the blurred stimulation was applied, PECAP detected an increase in current spread at the targeted central 'blurred' electrode compared to the current-spread estimate in the M_0 condition. No significant effects were observed for the current-spread estimates of non-target electrodes or for the neural-responsiveness estimate (Garcia et al., 2024).

PECAP has also been used to evaluate differences in current spread between differing electrode-array geometries. Cochlear-implant manufacturers have designed both 'straight' electrode arrays designed to be inserted next to the lateral wall of the cochlea's scala tympani, and 'perimodiolar' arrays that curve closer to the responsive neural tissue. In a large multi-centre dataset, no differences in current-spread were revealed between Advanced Bionics's (Valencia, California, USA) SlimJ and Mid-Scala arrays. However, Cochlear's (Sydney, Australia) Slim-Straight arrays showed decreased current spread compared with both the standard perimodiolar arrays (the Contour Advance series) and, to a greater extent, the Slim Modiolar arrays, with the strongest effect in the apical electrodes (Garcia & Carlyon, 2025). It was also observed that in the Cochlear dataset, for which computerised tomography (CT) scans were available and electrode-modiolus-distances (EMDs) were calculated using a technique described by Sismono et al. (2022), a similar trend was present, in which the slim-straight arrays demonstrated larger EMDs than the perimodiolar arrays. However, the effect was strongest in the middle of the arrays rather than at the apex, suggesting that the degree of current spread that is observed at the nerves along the modiolus is influenced by more than just the distance between the modiolus and the stimulating electrodes.

Due to the high potential for clinical relevance stemming from the evidence of PECAP's ability to detect

changes in neural responsiveness and current spread, while also separating these two aspects of the electrode-neuron interface, steps have been taken towards its clinical translation. Recording PECAP data from all electrodes of a Cochlear CI using the clinical software Custom Sound EP (CSEP) takes 35-45 minutes after identifying the current required to achieve the most comfortable level (MCL) for each electrode. This duration is prohibitively long to implement in a clinical setting and would require an additional ≈ 1 hour appointment, something many clinics do not have the capacity for. With this in mind, a more-efficient method called 'SpeedCAP' was developed to record all the ECAP measurements required for submission to the PECAP algorithm in only 8 minutes. This method demonstrated no additional error in M_0 matrices beyond that observed in repeat measurements using the standard recording technique, and additionally demonstrated similarly reliable measurements intra-operatively as post-operatively (Garcia et al., 2023). However, no evidence was found for consistent estimates of σ and η when using equal-current intra-operative SpeedCAP measurements compared to post-operative, equal-loudness SpeedCAP data (Garcia, 2022), suggesting that further investigation is necessary to assess the feasibility of using PECAP as a fully objective tool.

Another barrier to clinical translation of PECAP is that the process of estimating σ and η from M_0 thus far has been done with custom scripts written in MATLAB (Mathworks, Natick, MA, USA) that require programming expertise to use. Demonstration of clinical viability requires development of a system that is easily usable by clinicians such as audiologists. This article describes an online platform that was developed that not only allows PECAP data-collection through a simple user interface but also performs analysis of new data.

PECAP Web Application

The online implementation of PECAP can be found in the following link: <https://panoramic-ecap.mrc-cbu.cam.ac.uk/>. An 'Introduction' page describes how to use the two functional pages of the web application that can be accessed after registration.

The first functional page is the 'DAQ' (Data Acquisition) page (Figure 2). This page is designed for use in conjunction with CSEP, the clinical software compatible with CI devices from Cochlear that contain a cic4 chip. It contains two PDF files that can be

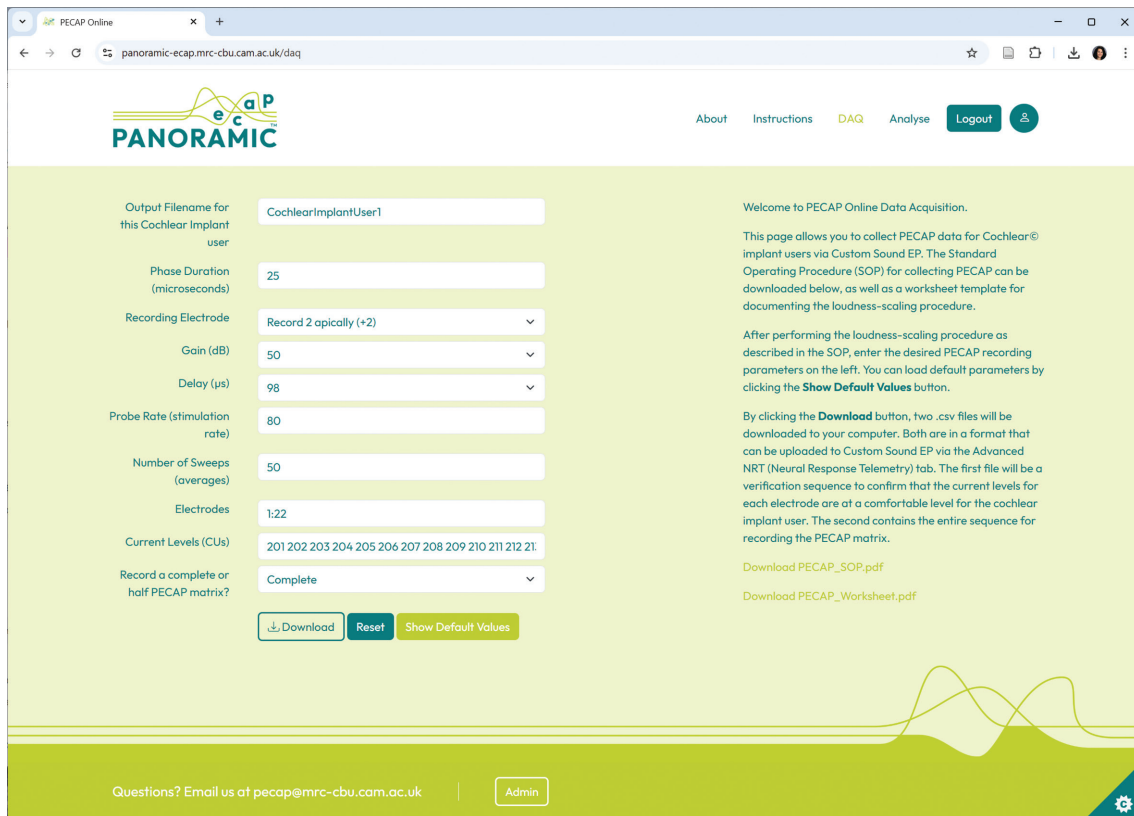


Figure 2. Data Acquisition (DAQ) page from the PECAP web application.

downloaded: an ‘SOP’ (Standard Operating Procedure) and a Worksheet for use in recording the current levels required for MCL from individual CI users. Users can follow the SOP and use the Worksheet to determine the parameters required for collecting PECAP from each new CI user. These parameters can then be entered into the fields on the DAQ page. Default values can be loaded by clicking ‘Show Default Values’, although ‘Current Levels (CUs)’ are unique to each CI user and must be updated. Clicking the ‘Download’ button generates a file in comma-separated values format (.csv) that is a configuration file for recording PECAP for the CI user in question. Uploading this .csv file to CSEP will enable users to record new M_0 data.

As recording the PECAP M_0 matrix requires the ability to record ECAPs using the forward-masking artefact-reduction technique, this functionality must be available in the clinical cochlear-implant software for it to be possible for users to measure PECAP in a clinical setting. Out of the three major cochlear-implant manufacturers, Cochlear is currently the only one that has this feature available in the clinical software. The DAQ page only enables PECAP data-collection for users of Cochlear CI devices. It is also possible to record M_0 in Cochlear, Advanced Bionics (AB), and

MEDEL (Innsbruck, Austria) CI devices using research software. Although this is not compatible with a clinical setting, M_0 can also be collected using Cochlear’s Nucleus Implant Communicator (NIC2; i.e. to record SpeedCAP), AB’s Bionic Ear Data Collection System (BEDCS), or using MEDEL’s Research Interface Box (RIB2). The AB implementation contains a graphical-user interface (GUI) that requires MATLAB but little programming experience to use. Code for collecting M_0 using the research platforms can be downloaded for Cochlear from https://github.com/charlottemgarcia/PECAP_PhD_Thesis (PECAP.py), and for AB from https://github.com/charlottemgarcia/PECAP_DataCollection. At the time of publication of this article, the MEDEL software (also containing a GUI and requiring no programming experience) is still under development.

The second functional page is the ‘Analyse’ page (Figure 3). This page is designed to analyse PECAP data collected using four different methods across cochlear-implant devices from both AB and Cochlear. Data-protection routines are in place within the website: any uploaded data are immediately pre-processed to extract M_0 , and the contents of the uploaded file are discarded and deleted prior to submission to the

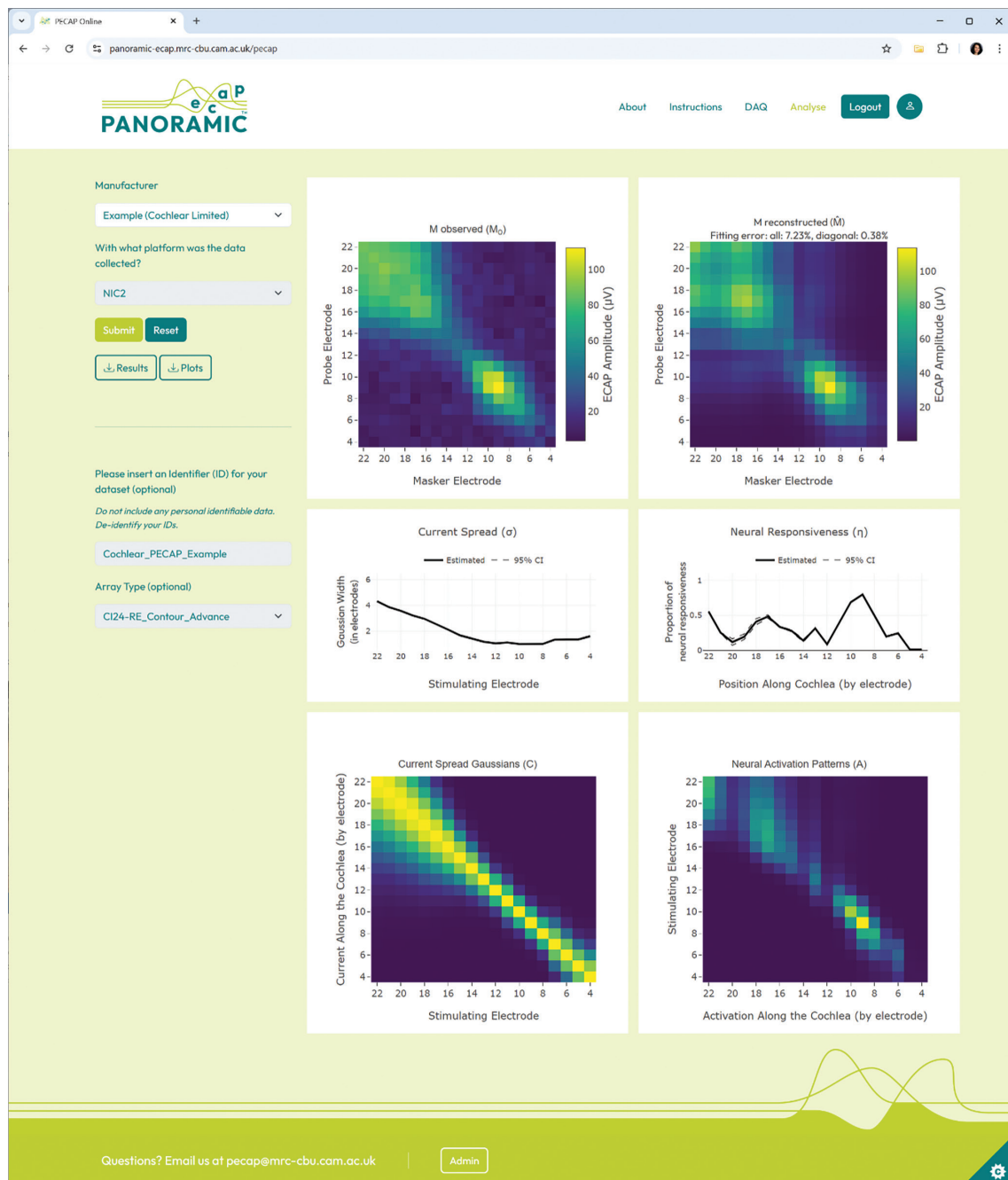


Figure 3. Analysis page from the PECAP web application with the results of an Example CI user with a Cochlear device where electrodes 1-3 were switched off in their clinical programme.

PECAP algorithm on a secure isolated server hosted at the University of Cambridge. Analysis outputs are not stored, therefore users must repeat the analysis if they do not save the results before navigating away from the webpage. It is also important to note that neither the uploaded data nor analysis outputs are ever saved within the web-app; all data are deleted immediately after analysis and cannot therefore be accessed by either website administrators or the host institution.

To analyse Cochlear data collected using the 'DAQ' page, users must select 'Cochlear Limited' in the 'Manufacturer' drop-down menu and 'Custom Sound EP (CSEP)' when asked 'With what platform was the data collected?' The 'Select the N1-P2 peak-picking procedure' feature allows users to decide whether to use the ECAP amplitudes calculated internally to the CSEP software ('replace invalid ECAPs with zeros'), or to run a peak-finding procedure for every cell of the M_0 matrix ('Calculate amplitude for every ECAP').

These approaches have different advantages: the former reduces the likelihood of the PECAP algorithm modelling noise, which sometimes results in higher, inaccurate current-spread estimates, particularly at either end of the electrode array. However, it may also remove cells from M_0 that represent genuine ECAP responses, thereby reducing the accuracy of both neural-responsiveness and current-spread estimates. Users must make a decision for each dataset using their own judgement.

The website also accepts PECAP data collected with Cochlear's research platform NIC2 and the scripts referenced above, as well as in the format generated by collecting data via the SpeedCAP method (Garcia et al., 2023). These options submit M_0 matrices that include an amplitude for every ECAP.

Finally, the website also processes AB PECAP data collected with BEDCS (version 1.18) and the scripts referenced above. Here, there is an option to smooth the ECAP waveforms using a 5-point running average to reduce system noise and avoid over-estimation of ECAP amplitudes prior to forming M_0 matrices from the data. While this can reduce noise, it should be used with caution, as it may also result in residual electrical artefacts being smoothed into the portion of the waveform where the neural response should be, therefore interfering with the ECAP amplitude estimation. Users should also indicate whether full or half M_0 matrices were recorded.

Once analysed, the PECAP results can be downloaded in both numerical and image formats. The system does not remove electrical artefacts, nor does it indicate whether the submitted data achieve the minimum 10 dB signal-to-noise ratio (SNR) required for accurate recreation of neural excitation patterns (Garcia et al., 2021). The SNR can be calculated using repeat measurements of M_0 or from the diagonal of M_0 . If this is not possible, a 'Fitting error: all' below $\approx 10\%$ and a maximum ECAP amplitude of at least ≈ 150 μV can be used as a proxy for the SNR criteria.

Conclusions

A web application has been developed that allows users to collect and analyse PECAP data to estimate individual patients' patterns of current spread and neural responsiveness in cochlear-implant users of Cochlear and Advanced-Bionics devices. Future upgrades will include compatibility with Cochlear's

NEXA platform. It will also be expanded to include compatibility with MEDEL devices, with data collection via the RIB2 research interface.

References

- Abbas, P. J., Brown, C. J., Shallop, J. K., Firszt, J. B., Hughes, M. L., Hong, S. H., & Staller, S. J. (1999). Summary of results using the nucleus CI24M implant to record the electrically evoked compound action potential. *Ear and Hearing*, 20(1), 45–59. <https://doi.org/10.1097/00003446-199902000-00005>
- Bierer, J. A. (2010). Probing the Electrode–Neuron Interface With Focused Cochlear Implant Stimulation. *Trends in Amplification*, 14(2), 84–95. <https://doi.org/10.1177/1084713810375249>
- Biesheuvel, J. D., Briaire, J. J., & Frijns, J. H. M. (2016). A Novel Algorithm to Derive Spread of Excitation Based on Deconvolution. *Ear and Hearing*, 37(5), 572. <https://doi.org/10.1097/AUD.0000000000000296>
- Blamey, P., Artieres, F., Başkent, D., Bergeron, F., Beynon, A., Burke, E., Dillier, N., Dowell, R., Fraysse, B., Gallégo, S., Govaerts, P. J., Green, K., Huber, A. M., Kleine-Punte, A., Maat, B., Marx, M., Mawman, D., Mosnier, I., O'Connor, A. F., ... Lazard, D. S. (2013). Factors affecting auditory performance of postlinguistically deaf adults using cochlear implants: An update with 2251 patients. *Audiology & Neuro-Otology*, 18(1), 36–47. <https://doi.org/10.1159/000343189>
- Brochier, T., Guérit, F., Deeks, J. M., Garcia, C., Bance, M., & Carlyon, R. P. (2021). Evaluating and Comparing Behavioural and Electrophysiological Estimates of Neural Health in Cochlear Implant Users. *JARO: Journal of the Association for Research in Otolaryngology*, 22(1), 67–80. <https://doi.org/10.1007/s10162-020-00773-0>
- Brown, C. J., Abbas, P. J., & Gantz, B. (1990). Electrically evoked whole-nerve action potentials: Data from human cochlear implant users. *The Journal of the Acoustical Society of America*, 88(3), 1385–1391. <https://doi.org/10.1121/1.399716>
- Carlyon, R. P., Cosentino, S., Deeks, J. M., Parkinson, W., & Arenberg, J. A. (2018). Effect of Stimulus Polarity on Detection Thresholds in Cochlear Implant Users: Relationships with Average Threshold, Gap Detection, and Rate Discrimination. *JARO: Journal of the Association for Research in Otolaryngology*, 19(5), 559–567. <https://doi.org/10.1007/s10162-018-0677-5>
- Charlet de Sauvage, R., Cazals, Y., Erre, J. P., & Aran, J. M. (1983). Acoustically derived auditory nerve action potential evoked by electrical stimulation: An estimation of the waveform of single unit contribution. *The Journal of the Acoustical Society of America*, 73(2), 616–627. <https://doi.org/10.1121/1.388872>
- Cohen, L. T., Richardson, L. M., Saunders, E., & Cowan, R. S. C. (2003). Spatial spread of neural excitation in cochlear implant recipients: Comparison of improved ECAP method and psychophysical forward masking. *Hearing Research*, 179(1), 72–87. [https://doi.org/10.1016/S0378-5955\(03\)00096-0](https://doi.org/10.1016/S0378-5955(03)00096-0)
- Cosentino, S., Gaudrain, E., Deeks, J. M., & Carlyon, R. P. (2015). Multistage Nonlinear Optimization to Recover Neural Activation Patterns From

- Evoked Compound Action Potentials of Cochlear Implant Users. *IEEE Transactions on Biomedical Engineering*, 63(4), 833–840. <https://doi.org/10.1109/TBME.2015.2476373>
- Davis, T. J., Zhang, D., Gifford, R. H., Dawant, B. M., Labadie, R. F., & Noble, J. H. (2016). Relationship Between Electrode-to-Modiolus Distance and Current Levels for Adults with Cochlear Implants. *Otology & Neurotology: Official Publication of the American Otological Society, American Neurotology Society [and] European Academy of Otology and Neurotology*, 37(1), 31–37. <https://doi.org/10.1097/MAO.0000000000000896>
- Dawson, P., Fullerton, A., Krishnamoorthi, H., Plant, K., Cowan, R., Buczak, N., Long, C. J., James, C. J., Sismono, F., & Büchner, A. (2025a, July). A prospective, multi-centre case-control trial examining factors that predict variable clinical performance in postlingual adult CI recipients (PREVA) [Poster]. Conference on Implantable Auditory Prostheses (CIAP).
- Dawson, P., Fullerton, A., Krishnamoorthi, H., Plant, K., Cowan, R., Buczak, N., Long, C., James, C. J., Sismono, F., & Büchner, A. (2025b). A Prospective, Multicentre Case-Control Trial Examining Factors That Explain Variable Clinical Performance in Post Lingual Adult CI Recipients. *Trends in Hearing*, 29, 23312165251347138. <https://doi.org/10.1177/23312165251347138>
- de Vos, J. J., Biesheuvel, J. D., Briaire, J. J., Boot, P. S., van Gendt, M. J., Dekkers, O. M., Fiocco, M., & Frijns, J. H. M. (2018). Use of Electrically Evoked Compound Action Potentials for Cochlear Implant Fitting: A Systematic Review. *Ear and Hearing*, 39(3), 401–411. <https://doi.org/10.1097/AUD.0000000000000495>
- DeVries, L., Schepeler, R., & Bierer, J. A. (2016). Assessing the Electrode-Neuron Interface with the Electrically Evoked Compound Action Potential, Electrode Position, and Behavioral Thresholds. *JARO: Journal of the Association for Research in Otolaryngology*, 17(3), 237–252. <https://doi.org/10.1007/s10162-016-0557-9>
- Firszt, J. B., Holden, L. K., Skinner, M. W., Tobey, E. A., Peterson, A., Gagg, W., Runge-Samuels, C. L., & Wackym, P. A. (2004). Recognition of speech presented at soft to loud levels by adult cochlear implant recipients of three cochlear implant systems. *Ear and Hearing*, 25(4), 375–387. <https://doi.org/10.1097/01.aud.0000134552.22205.ee>
- Friesen, L. M., Shannon, R. V., Baskent, D., & Wang, X. (2001). Speech recognition in noise as a function of the number of spectral channels: Comparison of acoustic hearing and cochlear implants. *The Journal of the Acoustical Society of America*, 110(2), 1150–1163. <https://doi.org/10.1121/1.1381538>
- Garcia, C. (2022). *The Panoramic ECAP Method: Estimating patient-specific patterns of current spread and neural health in cochlear-implant users*. <https://www.repository.cam.ac.uk/handle/1810/341691>
- Garcia, C., & Carlyon, R. P. (2025). Assessing Array-Type Differences in Cochlear Implant Users Using the Panoramic ECAP Method. *Ear and Hearing*, 46(5), 1355. <https://doi.org/10.1097/AUD.0000000000001673>
- Garcia, C., Deeks, J. M., Goehring, T., Borsetto, D., Bance, M., & Carlyon, R. P. (2023). SpeedCAP: An Efficient Method for Estimating Neural Activation Patterns Using Electrically Evoked Compound Action-Potentials in Cochlear Implant Users. *Ear and Hearing*, 44(3), 627. <https://doi.org/10.1097/AUD.0000000000001305>
- Garcia, C., Goehring, T., Cosentino, S., Turner, R. E., Deeks, J. M., Brochier, T., Rughooputh, T., Bance, M., & Carlyon, R. P. (2021). The Panoramic ECAP Method: Estimating Patient-Specific Patterns of Current Spread and Neural Health in Cochlear Implant Users. *Journal of the Association for Research in Otolaryngology: JARO*, 22(5), 567–589. <https://doi.org/10.1007/s10162-021-00795-2>
- Garcia, C., Morse-Fortier, C., Guérit, F., Hislop, S., Goehring, T., Carlyon, R. P., & Arenberg, J. G. (2024). Investigating the Effect of Blurring and Focusing Current in Cochlear Implant Users with the Panoramic ECAP Method. *Journal of the Association for Research in Otolaryngology*, 25(6), 591–609. <https://doi.org/10.1007/s10162-024-00966-x>
- Garcia, C., Sismono, F., Goehring, T., Guérit, F., Arzounian, D., & Carlyon, R. P. (2025). A comparison of electrophysiological measures for characterizing the cochlear-implant electrode-neuron interface. *JASA Express Letters*, 5(8), 082001. <https://doi.org/10.1121/10.0038746>
- Goehring, T., Archer-Boyd, A. W., Arenberg, J. G., & Carlyon, R. P. (2021). The effect of increased channel interaction on speech perception with cochlear implants. *Scientific Reports*, 11(1), Article 1. <https://doi.org/10.1038/s41598-021-89932-8>
- Goehring, T., Arenberg, J. G., & Carlyon, R. P. (2020). Using Spectral Blurring to Assess Effects of Channel Interaction on Speech-in-Noise Perception with Cochlear Implants. *JARO: Journal of the Association for Research in Otolaryngology*, 21(4), 353–371. <https://doi.org/10.1007/s10162-020-00758-z>
- Goldwyn, J. H., Bierer, S. M., & Bierer, J. A. (2010). Modeling the electrode-neuron interface of cochlear implants: Effects of neural survival, electrode placement, and the partial tripolar configuration. *Hearing Research*, 268(1–2), 93–104. <https://doi.org/10.1016/j.heares.2010.05.005>
- He, S., Shahsavarani, B. S., McFayden, T. C., Wang, H., Gill, K. E., Xu, L., Chao, X., Luo, J., Wang, R., & He, N. (2018). Responsiveness of the Electrically Stimulated Cochlear Nerve in Children with Cochlear Nerve Deficiency. *Ear and Hearing*, 39(2), 238–250. <https://doi.org/10.1097/AUD.0000000000000467>
- Holden, L. K., Finley, C. C., Firszt, J. B., Holden, T. A., Brenner, C., Potts, L. G., Gotter, B. D., Vanderhoof, S. S., Mispagel, K., Heydebrand, G., & Skinner, M. W. (2013). Factors Affecting Open-Set Word Recognition in Adults With Cochlear Implants. *Ear & Hearing*, 34(3), 342–360. <https://doi.org/10.1097/AUD.0b013e3182741aa7>
- Hrncirik, F., Roberts, I. V., Swords, C., Christopher, P. J., Chhabu, A., Gee, A. H., & Bance, M. L. (2022). Impact of Scala Tympani Geometry on Insertion Forces during Implantation. *Biosensors*, 12(11), 999. <https://doi.org/10.3390/bios12110999>
- Hughes, M. L., & Stille, L. J. (2010). Effect of stimulus and recording parameters on spatial spread of excitation and masking patterns obtained with the electrically evoked compound action potential in cochlear implants. *Ear and Hearing*, 31(5), 679–692. <https://doi.org/10.1097/AUD.0b013e3181e1d19e>
- Jwair, S., Prins, A., Wegner, I., Stokroos, R. J., Versnel, H., & Thomeer, H. G. X. M. (2021). Scalar Translocation Comparison Between Lateral Wall

- and Perimodiolar Cochlear Implant Arrays—A Meta-Analysis. *The Laryngoscope*, 131(6), 1358–1368. <https://doi.org/10.1002/lary.29224>
- Jwair, S., Versnel, H., Stokroos, R. J., & Thomeer, H. G. X. M. (2022). The effect of the surgical approach and cochlear implant electrode on the structural integrity of the cochlea in human temporal bones. *Scientific Reports*, 12(1), 17068. <https://doi.org/10.1038/s41598-022-21399-7>
- Kalkman, R. K., Briaire, J. J., Dekker, D. M. T., & Frijns, J. H. M. (2022). The relation between polarity sensitivity and neural degeneration in a computational model of cochlear implant stimulation. *Hearing Research*, 415, 108413. <https://doi.org/10.1016/j.heares.2021.108413>
- Kim, J.-R., Tejani, V. D., Abbas, P. J., & Brown, C. J. (2017). Intracochlear Recordings of Acoustically and Electrically Evoked Potentials in Nucleus Hybrid L24 Cochlear Implant Users and Their Relationship to Speech Perception. *Frontiers in Neuroscience*, 11. <https://doi.org/10.3389/fnins.2017.00216>
- Konerding, W., Arenberg, J., Sznabel, D., Kral, A., & Baumhoff, P. (2025). An Electrically Evoked Compound Action Potential Marker for Local Spiral Ganglion Neuron Degeneration: The Failure Index. *Journal of Neuroscience*, 45(7). <https://doi.org/10.1523/JNEUROSCI.0954-24.2024>
- Lazard, D. S., Vincent, C., Venail, F., Van de Heyning, P., Truy, E., Sterkers, O., Skarzynski, P. H., Skarzynski, H., Schauwers, K., O'Leary, S., Mawman, D., Maat, B., Kleine-Punte, A., Huber, A. M., Green, K., Govaerts, P. J., Fraysse, B., Dowell, R., Dillier, N., ... Blamey, P. J. (2012). Pre-, per- and postoperative factors affecting performance of postlinguistically deaf adults using cochlear implants: A new conceptual model over time. *PloS One*, 7(11), e48739. <https://doi.org/10.1371/journal.pone.0048739>
- McKay, C. M., Chandan, K., Akhoun, I., Siciliano, C., & Kluk, K. (2013). Can ECAP Measures Be Used for Totally Objective Programming of Cochlear Implants? *JARO: Journal of the Association for Research in Otolaryngology*, 14(6), 879–890. <https://doi.org/10.1007/s10162-013-0417-9>
- Mewes, A., Bennett, C., Dambon, J., Brademann, G., & Hey, M. (2023). Evaluation of CI electrode position from imaging: Comparison of an automated technique with the established manual method. *BMC Medical Imaging*, 23(1), 143. <https://doi.org/10.1186/s12880-023-01102-6>
- Moyaert, J., Gilles, A., Ramekers, D., Mertens, G., Fransen, E., Cardon, E., Biot, L., Verhelst, E., Van Rompaey, V., & Lammers, M. J. (2025). Cochlear health in a cohort of cochlear implant users carrying the p.Pro51Ser variant in the COCH gene (DFNA9): A cross-sectional study evaluating the changes in the electrically evoked compound action potential (eCAP). *Hearing Research*, 460, 109240. <https://doi.org/10.1016/j.heares.2025.109240>
- Mudry, A., & Mills, M. (2013). The Early History of the Cochlear Implant: A Retrospective. *JAMA Otolaryngology–Head & Neck Surgery*, 139(5), 446–453. <https://doi.org/10.1001/jamaoto.2013.293>
- Peng, T., Garcia, C., Haneman, M., Shader, M. J., Carlyon, R. P., & McKay, C. M. (2025). Comparing Patient-Specific Variations in Intra-Cochlear Neural Health Estimated Using Psychophysical Thresholds and Panoramic Electrically Evoked Compound Action Potentials (PECAPs). *Journal of the Association for Research in Otolaryngology: JARO*, 26(1), 77–91. <https://doi.org/10.1007/s10162-024-00972-z>
- Pfingst, B. E., Zhou, N., Colesa, D. J., Watts, M. M., Strahl, S. B., Garadat, S. N., Schwartz-Leyzac, K. C., Budenz, C. L., Raphael, Y., & Zwolan, T. A. (2015). Importance of cochlear health for implant function. *Hearing Research*, 322, 77–88. <https://doi.org/10.1016/j.heares.2014.09.009>
- Prado-Guitierrez, P., Fewster, L. M., Heasman, J. M., McKay, C. M., & Shepherd, R. K. (2006). Effect of interphase gap and pulse duration on electrically evoked potentials is correlated with auditory nerve survival. *Hearing Research*, 215(1–2), 47–55. <https://doi.org/10.1016/j.heares.2006.03.006>
- Ramekers, D., Benav, H., Klis, S. F. L., & Versnel, H. (2022). Changes in the Electrically Evoked Compound Action Potential over time After Implantation and Subsequent Deafening in Guinea Pigs. *Journal of the Association for Research in Otolaryngology*, 23(6), 721–738. <https://doi.org/10.1007/s10162-022-00864-0>
- Ramekers, D., Versnel, H., Strahl, S. B., Smeets, E. M., Klis, S. F. L., & Grolman, W. (2014). Auditory-nerve responses to varied inter-phase gap and phase duration of the electric pulse stimulus as predictors for neuronal degeneration. *Journal of the Association for Research in Otolaryngology: JARO*, 15(2), 187–202. <https://doi.org/10.1007/s10162-013-0440-x>
- Sismono, F., Leblans, M., Mancini, L., Veneziano, A., Zanini, F., Dirckx, J., Bernaerts, A., de Foer, B., Offeciers, E., & Zarowski, A. (2022). 3D-localisation of cochlear implant electrode contacts in relation to anatomical structures from in vivo cone-beam computed tomography. *Hearing Research*, 426, 108537. <https://doi.org/10.1016/j.heares.2022.108537>
- Skidmore, J., Xu, L., Chao, X., Riggs, W. J., Pellitteri, A., Vaughan, C., Ning, X., Wang, R., Luo, J., & He, S. (2021). Prediction of the Functional Status of the Cochlear Nerve in Individual Cochlear Implant Users Using Machine Learning and Electrophysiological Measures. *Ear and Hearing*, 42(1), 180. <https://doi.org/10.1097/AUD.0000000000000916>
- Swords, C. (2024). *Anatomical and Electrical Characterisation of The Human Cochlea Towards the Improvement of Cochlear Implant Performance*. <https://doi.org/10.17863/CAM.112673>
- Wanna, G. B., Noble, J. H., Carlson, M. L., Gifford, R. H., Dietrich, M. S., Haynes, D. S., Dawant, B. M., & Labadie, R. F. (2014). Impact of electrode design and surgical approach on scalar location and cochlear implant outcomes. *The Laryngoscope*, 124 Suppl 6(0 6), S1-7. <https://doi.org/10.1002/lary.24728>
- Wu, P. Z., Liberman, L. D., Bennett, K., de Gruttola, V., O'Malley, J. T., & Liberman, M. C. (2019). Primary Neural Degeneration in the Human Cochlea: Evidence for Hidden Hearing Loss in the Aging Ear. *Neuroscience, Hearing Loss, Tinnitus, Hyperacusis, Central Gain*, 407, 8–20. <https://doi.org/10.1016/j.neuroscience.2018.07.053>
- Zeng, F.-G. (2022). Celebrating the one millionth cochlear implant. *JASA Express Letters*, 2(7), 077201. <https://doi.org/10.1121/10.0012825>
- Zhou, N., & Pfingst, B. E. (2014). Relationship between multipulse integration and speech recognition with cochlear implants. *The Journal of the Acoustical Society of America*, 136(3), 1257–1268. <https://doi.org/10.1121/1.4890640>

Acknowledgements

This work was funded by an Early Career Researcher award from the Centre for Integrative Neuroscience Discovery at the University of Cambridge, and by an Impact Acceleration Award (No. G116517) from the United Kingdom Research and Innovation's Medical Research Council. The author would additionally like to thank Tomas Lazauskas (The Alan Turing Institute) who conducted the software development for the back-end of the web application, and Alaa Marouf (AM Branding Ltd) who developed the branding and graphic design for the front-end of the online platform.

Conflict of interest

The author has no conflicts of interest, financial or otherwise, to disclose. No Artificial Intelligence was used in the generation of this article.

Editorial Office

Edited by: Rita López

Production: GlauX Publicaciones Académicas